

Guinea Fowl Coronavirus Diversity Has Phenotypic Consequences for Glycan and Tissue Binding

Kim M Bouwman, Mattias Delpont, Frederik Broszeit, Renaud Berger, Erik a W S Weerts, Marie-Noêlle Lucas, Maxence Delverdier, Sakhia Belkasmi, Andreas Papanikolaou, Geert-Jan Boons, et al.

▶ **To cite this version:**

Kim M Bouwman, Mattias Delpont, Frederik Broszeit, Renaud Berger, Erik a W S Weerts, et al.. Guinea Fowl Coronavirus Diversity Has Phenotypic Consequences for Glycan and Tissue Binding. Journal of Virology, 2019, 93 (10), 10.1128/JVI.00067-19 . hal-02947431v2

HAL Id: hal-02947431
https://hal.inrae.fr/hal-02947431v2

Submitted on 7 May 2021

HAL is a multi-disciplinary open access archive for the deposit and dissemination of scientific research documents, whether they are published or not. The documents may come from teaching and research institutions in France or abroad, or from public or private research centers.

L'archive ouverte pluridisciplinaire **HAL**, est destinée au dépôt et à la diffusion de documents scientifiques de niveau recherche, publiés ou non, émanant des établissements d'enseignement et de recherche français ou étrangers, des laboratoires publics ou privés.



Distributed under a Creative Commons Attribution 4.0 International License

AMERICAN SOCIETY FOR MICROBIOLOGY | Journal of Virology®

VIRUS-CELL INTERACTIONS

Guinea Fowl Coronavirus Diversity Has Phenotypic Consequences for Glycan and Tissue Binding

Kim M. Bouwman,[a] Mattias Delpont,[b] Frederik Broszeit,[c] Renaud Berger,[b] Erik A. W. S. Weerts,[a] Marie-Noëlle Lucas,[b] Maxence Delverdier,[b] Sakhia Belkasmi,[b] Andreas Papanikolaou,[a] Geert-Jan Boons,[c] Jean-Luc Guérin,[b] Robert P. de Vries,[c] Mariette F. Ducatez,[b] Monique H. Verheije[a]

[a]Department of Pathobiology, Faculty of Veterinary Medicine, Utrecht University, Utrecht, The Netherlands
[b]IHAP, Université de Toulouse, INRA, ENVT, Toulouse, France
[c]Department of Chemical Biology and Drug Discovery, Utrecht Institute for Pharmaceutical Sciences, Utrecht University, Utrecht, The Netherlands

ABSTRACT Guinea fowl coronavirus (GfCoV) causes fulminating enteritis that can result in a daily death rate of 20% in guinea fowl flocks. Here, we studied GfCoV diversity and evaluated its phenotypic consequences. Over the period of 2014 to 2016, affected guinea fowl flocks were sampled in France, and avian coronavirus presence was confirmed by PCR on intestinal content and immunohistochemistry of intestinal tissue. Sequencing revealed 89% amino acid identity between the viral attachment protein S1 of GfCoV/2014 and that of the previously identified GfCoV/2011. To study the receptor interactions as a determinant for tropism and pathogenicity, recombinant S1 proteins were produced and analyzed by glycan and tissue arrays. Glycan array analysis revealed that, in addition to the previously elucidated biantennary di-*N*-acetyllactosamine (diLacNAc) receptor, viral attachment S1 proteins from GfCoV/2014 and GfCoV/2011 can bind to glycans capped with alpha-2,6-linked sialic acids. Interestingly, recombinant GfCoV/2014 S1 has an increased affinity for these glycans compared to that of GfCoV/2011 S1, which was in agreement with the increased avidity of GfCoV/2014 S1 for gastrointestinal tract tissues. Enzymatic removal of receptors from tissues before application of spike proteins confirmed the specificity of S1 tissue binding. Overall, we demonstrate that diversity in GfCoV S1 proteins results in differences in glycan and tissue binding properties.

IMPORTANCE Avian coronaviruses cause major global problems in the poultry industry. As causative agents of huge economic losses, the detection and understanding of the molecular determinants of viral tropism are of ultimate importance. Here, we set out to study those parameters and obtained in-depth insight into the virus-host interactions of guinea fowl coronavirus (GfCoV). Our data indicate that diversity in GfCoV viral attachment proteins results in differences in degrees of affinity for glycan receptors, as well as altered avidity for intestinal tract tissues, which might have consequences for GfCoV tissue tropism and pathogenesis in guinea fowls.

KEYWORDS coronavirus, glycan receptor, guinea fowl, receptor affinity, spike protein, tissue tropism

Avian coronaviruses (AvCoVs) pose a major threat to poultry health, production, and welfare worldwide. AvCoVs are highly infectious, remain endemic in poultry populations, and, due to their high mutation rate, frequently produce new antigenic variants (1, 2). The best-known AvCoV is infectious bronchitis virus (IBV), causing mainly respiratory disease in chickens. In addition, IBV-like viruses have been detected in other domestic poultry, including turkey and quail (3–5). In guinea fowl, coronaviruses were identified for the first time in 2011 as the causative agent for fulminating enteritis (6). Full-genome sequencing revealed that guinea fowl coronavirus GfCoV/FR/2011 is

Citation Bouwman KM, Delpont M, Broszeit F, Berger R, Weerts EAWS, Lucas M-N, Delverdier M, Belkasmi S, Papanikolaou A, Boons G-J, Guérin J-L, de Vries RP, Ducatez MF, Verheije MH. 2019. Guinea fowl coronavirus diversity has phenotypic consequences for glycan and tissue binding. J Virol 93:e00067-19. https://doi.org/10.1128/JVI.00067-19.

Editor Tom Gallagher, Loyola University Chicago

Copyright © 2019 Bouwman et al. This is an open-access article distributed under the terms of the Creative Commons Attribution 4.0 International license.

Address correspondence to Mariette F. Ducatez, m.ducatez@envt.fr, or Monique H. Verheije, m.h.verheije@uu.nl.

Received 17 January 2019
Accepted 20 February 2019
Accepted manuscript posted online 6 March 2019
Published 1 May 2019

Downloaded from http://jvi.asm.org/ on April 22, 2021 at INRAE - Inst Natl de Rech pour l'Agriculture, l'Alimentation et l'Environnement

closely associated with turkey coronavirus (TCoV) (7), with both causing gastrointestinal tract infections in their respective hosts (6, 8). Clinical signs related to GfCoV infection in guinea fowl include prostration, ruffled feathers, and decreased water and feed consumption, and GfCoV infection has resulted in a daily death rate of up to 20% in several farms in France (6). Upon necropsy of affected animals, whitish and enlarged pancreases were consistently reported. Histopathological analyses revealed pancreatic necrosis and lesions of various intensities in the intestinal epithelium, with the most severe lesions found in the duodenum of affected animals (6).

Genetic classification of AvCoVs is based on phylogenetic analysis of the S1 domain of its viral attachment protein spike (2). The spike protein is the main determinant for tropism (9), and the N-terminal part of the S1 of IBV has been shown to contain the receptor-binding domain (RBD) (10). Studies using recombinant IBV S1 and/or RBD proteins have demonstrated that the viral tropism is reflected by tissue binding of such proteins (11). Mutations in the spike proteins of IBV might result in either decreased (10) or increased (12) avidity for its receptor present on epithelial cells of the chicken trachea. In contrast to IBV, GfCoV and TCoV target the epithelial cells of the gastrointestinal tract (4, 6), and recombinant protein binding of their S1 proteins reflects this viral tropism, with predominant staining of epithelial cells of the small intestine (4). Glycan array analysis identified elongated biantennary *N*-acetyllactosamine (di-LacNAc) molecules on N-glycans as the host receptor for enteric AvCoVs, which are abundantly expressed on intestinal tissues (4).

Clinical symptoms in guinea fowl similar to those reported in 2011 are continuously reported by veterinarians in France (personal communication). However, studies on newly emerging GfCoVs are particularly hampered by the lack of models to grow the virus. More specifically, susceptible cell lines have not yet been identified, inoculation of embryonated guinea fowl eggs did not result in GfCoV production (data not shown), and specific-pathogen-free (SPF) guinea fowls are not available for experimental infection.

Here, we set out to study the consequences of GfCoV genetic diversity for glycan and tissue interactions. We revealed that the GfCoV spike gene from the 2014–2016 outbreak in guinea fowl flocks in France was 89% identical to that of GfCoV/2011 (7). Glycan and tissue binding analyses of GfCoV/2011 and GfCoV/2014 recombinant spike S1 proteins revealed that while both proteins had the same specificities, GfCoV/2014 S1 had a much higher affinity toward glycan receptors and tissues of the lower gastrointestinal tract, in agreement with the observed replication of the virus in these tissues from field cases. Taking these observations together, we demonstrate that GfCoV diversity results in phenotypically different receptor binding properties.

RESULTS

Lesions and coronaviral protein expression in the gastrointestinal tract of diseased guinea fowls between 2014 and 2016. Fulminating disease (peracute enteritis) in guinea flocks continued to be reported after the initial outbreak of GfCoV infection in 2011 (6). Between February 2014 and November 2016, duodena from 29 diseased guinea fowls were collected and analyzed for lesions and coronaviral protein expression. Histological analysis of tissues by hematoxylin and eosin (H&E) staining revealed lesions in all duodena, with clear infiltration of inflammatory cells in remnants of the villi (Fig. 1, black arrowheads). For seven animals, the entire gastrointestinal tract was available for histological analysis, showing lesions across the entire length of the intestinal tract, including the colon (Fig. 1, black arrowheads). Viral protein expression using antibodies against the M protein of avian coronaviruses was observed in all duodena and in four out of the seven lower intestinal tracts by immunohistochemistry (IHC) (Fig. 1, white arrowheads). In the colons devoid of expression of viral proteins, the infiltration of inflammatory cells was noted, suggestive of a previous exposure to a virologic agent.

In contrast to what we observed, virus replication of GfCoV/2011 appeared to be restricted to the duodenum (6). Unfortunately, we were unable to confirm the lack of

Downloaded from http://jvi.asm.org/ on April 22, 2021 at INRAE - Inst Natl de Rech pour l'Agriculture, l'Alimentation et l'Environnement

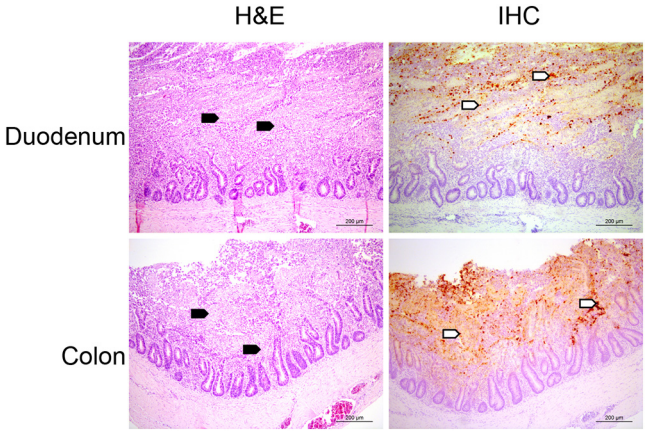


FIG 1 (Immuno)histological analyses of guinea fowl intestinal tract. Shown are representative images of duodenum and colon from a guinea fowl presenting with peracute enteritis in 2014 after samples were stained with H&E or antibodies against the M protein of infectious bronchitis virus, known to cross-react with GfCoV M protein in immunohistochemistry (IHC). Black arrowheads indicate inflammatory cells, and white arrowheads indicate viral protein expression.

infection of lower gastrointestinal tract samples in the previous outbreak due to unavailability of samples. Nevertheless, we here hypothesize that genetically divergent GfCoVs might have caused phenotypic differences in guinea fowls over the years.

Circulation of genetically diverse GfCoV. Gastrointestinal content collected from 20 affected animals between February 2014 and November 2016 was analyzed for the presence of gammacoronavirus genetic material by one-step real-time reverse transcription-PCR (RT-PCR) using pan-gammacoronavirus primers (13). For all samples, threshold cycle (C_T) values obtained were below 35 (data not shown), confirming the presence of coronaviral RNA in all tested samples (Table 1). Next, overlapping conventional PCRs were performed with primers based on the spike gene of the GfCoV/2011 virus (sequences available upon request). Partial S1 sequences could be obtained from 10 of 20 RT-PCR-positive samples (893 to 1,841 nucleotides [nt]; 3,624 nt in the complete S sequence) (Table 1); the quality and/or quantity of the remaining 10 samples was too low to generate PCR products. Sanger sequencing of the obtained

TABLE 1 Overview of selected guinea fowls and obtained GfCoV spike sequences

Animal no.[a]	Date of sample collection (wk no./yr)	Age at sampling time (wk)[b]	GenBank accession no. (spike sequence [nt])	% nucleotide identity with GfCoV/2011 S1[c]
14-002	6/2014	10		
14-013	15/2014	8		
14-032	22/2014	7	MG765535 (1–3669)	85
14-036	24/2014	7		
14-037	25/2014	7		
14-039	26/2014	5.5		
14-040	23/2014	ND	MG765536 (1–1392)	88
14-041	23/2014	ND	MG765537 (1–1771)	88
14-042	23/2014	ND	MG765538 (1–1392)	88
14-047	33/2014	3	MG765539 (1–1378)	88
14-053	37/2014	9	MG765540 (1–1393)	88
14-065	44/2014	12		
14-066	45/2014	4	MG765541 (1–1384)	88
15-006	3/2015	ND	MG765542 (1–980)	87
15-116	46/2015	7		
15-118	47/2015	8		
16-086	38/2016	ND	MK290733 (1–2465)	85
16-115	45/2016	4		
16-123	47/2016	ND	MK290734 (571–1895)	86

[a]Animals identified by boldface numbers were included for immunohistological examination as well.
[b]ND, not determined.
[c]Based on the S1 sequence (nt 1 to 3708) of GfCov/FR/2011, GenBank accession number LN610099.1.

Downloaded from http://jvi.asm.org/ on April 22, 2021 at INRAE - Inst Natl de Rech pour l'Agriculture, l'Alimentation et l'Environnement

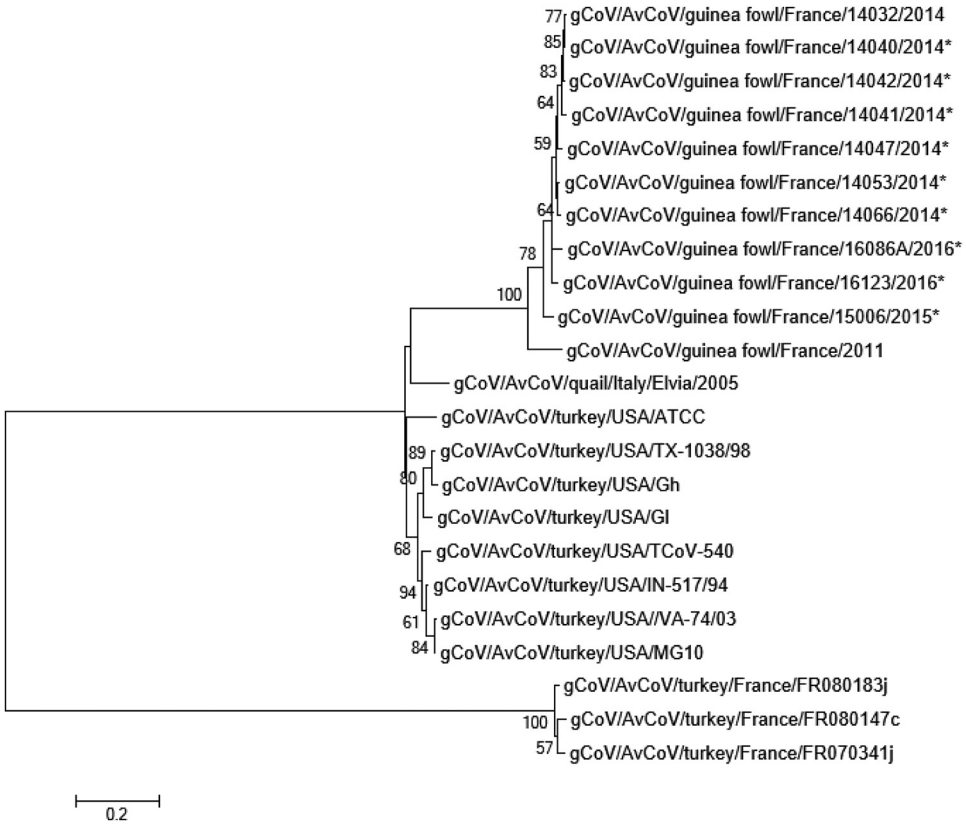


FIG 2 Molecular phylogenetic analysis by maximum likelihood method comparing GfCoV (partial) spike sequences. Phylogenetic tree was based on the Kimura two-parameter model, in which bootstrap values are shown next to the branches. The analysis involved 22 nucleotide sequences. All positions containing gaps and missing data were eliminated. There were a total of 893 nucleotide positions in the final data set. Evolutionary analyses were conducted in MEGA, version 6. *, partial S1 sequence of GfCoV.

fragments confirmed the presence of GfCoV in the intestinal content of all 10 birds, confirming continuous GfCoV circulation in France.

Phylogenetic analysis was performed to investigate the genetic diversity of the obtained partial S1 sequences using maximum likelihood analyses (Fig. 2). The results showed that the 2014–2016 sequences clearly clustered with the S1 reference gene from GfCoV/2011 (GenBank accession number HF544506) supported by a bootstrap value of 100, while they were genetically more distantly related to TCoV. Each of the GfCoV 2014–2016 partial S1 sequences shared 85% to 88% nucleotide identity with the GfCoV/2011 S1 sequence, and between the 2014 and 2016 partial S1 sequences, the variation was 0.1 to 8.0%.

Only from one sample could a full spike sequence be obtained (γCoV/AvCoV/guinea fowl/France/14032/2014) while for the other samples the amount and/or quality of the viral RNA samples was too low for further analyses. Comparison of the S1 gene of GfCoV/2014 with that of GfCoV/2011 using the Kimura two-parameter distance model indicated that the genes had an 85% nucleotide and an 89% amino acid sequence identity. Alignment of the amino acid sequences did not indicate clear mutation hot spots (data not shown), and the huge sequence diversity with the S1 of IBV strain M41 (the only avian coronavirus for which a cryo-electron microscopy [cryo-EM] structure has been elucidated [14]) precluded further suggestions on the implications of each of the mutations.

GfCoV/2014 S1 recognizes the enteric coronavirus diLacNAc glycan receptor with higher affinity than GfCoV/2011 S1. Using the glycan array of the Consortium for Functional Glycomics, we previously determined that S1 from GfCoV/2011 specifically binds to the diLacNAc glycan receptors (Galβ1,4GlcNAcβ1,3Galβ1,4GlcNAc) (4). To

Downloaded from http://jvi.asm.org/ on April 22, 2021 at INRAE - Inst Natl de Rech pour l'Agriculture, l'Alimentation et l'Environnement

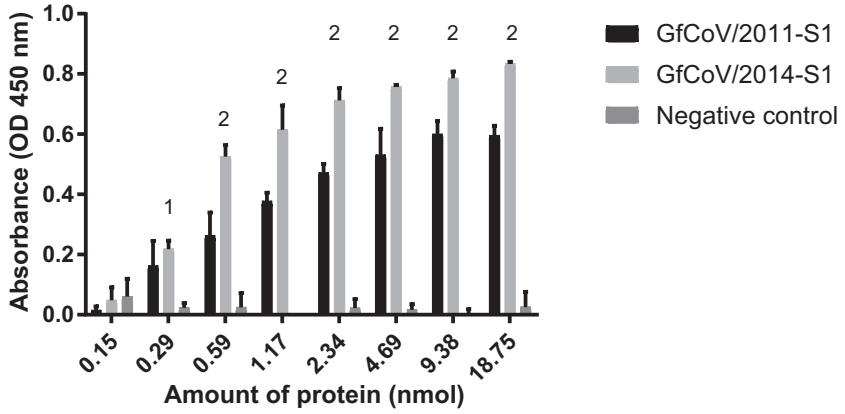


FIG 3 Binding of GfCoV S1 to the enteric coronavirus glycan receptor diLacNAc. Concentration-dependent binding of GfCoV S1 proteins to Galβ1,4GlcNAcβ1,3Galβ1,4GlcNAc in ELISA. The N-terminal domain of the S1 protein of IBV strain M41 was used as a negative control (10). 1, significant difference between GfCoV S1 and IBV-M41; 2, significant difference between GfCoV/2014 S1 and GfCoV/2011 S1 ($P < 0.001$).

study whether the observed changes in the spike of GfCoV/2014 resulted in differences in recognition of this glycan receptor, we recombinantly produced GfCoV/2014 S1 and GfCoV/2011 S1 and applied both proteins to diLacNAc-polyacrylic acid (PAA) conjugates in an enzyme-linked immunosorbent assay (ELISA) as previously described (4). At similar protein concentrations, GfCoV/2014 S1 showed improved binding to this receptor (Fig. 3), indicating that the mutations in S1 did not affect the specificity but resulted in significantly higher affinity for this particular receptor.

The genetic differences between GfCoV/2014 and GfCoV/2011 did not alter glycan specificity. Next, we investigated whether the mutations in S1 resulted in recognition of additional N-linked glycans. To this end, both S1 proteins were applied to a novel glycan array containing N-glycan structures with their linear counterparts, either with terminal galactose or two differently linked sialic acid moieties (F. Broszeit and R. P. de Vries, submitted for publication). Schematic representations of each of the glycans are given in Fig. 4A. The data revealed that both GfCoV S1 proteins bind to longer biantennary LacNAc structures (Fig. 4B, structures 3 and 4), including the diLacNAc structure used in the ELISA (Fig. 3). Furthermore, both GfCoV S1 proteins bound to longer linear LacNAc repeats (Fig. 4B, structure 1), which were not included in the previous array (4). Finally, both GfCoV S1 proteins bound longer linear and biantennary LacNAc repeats with terminal alpha-2,6 sialic acid (Fig. 4B, structures 9 to 12) but not those capped with alpha-2,3-linked sialic acids (Fig. 4B, structures 5 to 8). *Erythrina crista-galli* lectin (ECA), *Sambucus nigra* lectin (SNA), and *Maackia Amurensis* lectin I (MAL1) were used as controls. We observed, as expected, specific binding to galactose and alpha-2,6-linked and alpha-2,3-linked sialic acid terminal glycans, respectively (Fig. 4C). In conclusion, both GfCoV S1 proteins show specificity for the same glycans, ending with either galactose or alpha-2,6-linked sialic acids on the glycan array. However, the relative fluorescence observed for GfCoV/2014 S1 was consistently higher than that for GfCoV/2011 S1, which is suggestive of differences in their affinities for glycan receptors, as observed for diLacNAcs in the data shown in Fig. 3.

GfCoV/2014 S1 has higher affinity for glycan receptors than GfCoV/2011 S1. To allow comparison of the binding affinities of the two proteins for each glycan, we applied 5-fold serial S1 protein dilutions onto the glycan array and compared binding intensities at various scan powers. At each concentration, for all glycans shown in Fig. 4A, binding signals of GfCoV/2014 S1 (Fig. 5A) were consistently higher than those of GfCoV/2011 S1 (Fig. 5B). Detection of linear glycan binding (glycans 1 and 9) required higher concentrations and scan powers than the detection of biantennary LacNAc structures (glycans 3 and 4 and glycans 11 and 12) for both proteins. Interestingly,

Downloaded from http://jvi.asm.org/ on April 22, 2021 at INRAE - Inst Natl de Rech pour l'Agriculture, l'Alimentation et l'Environnement

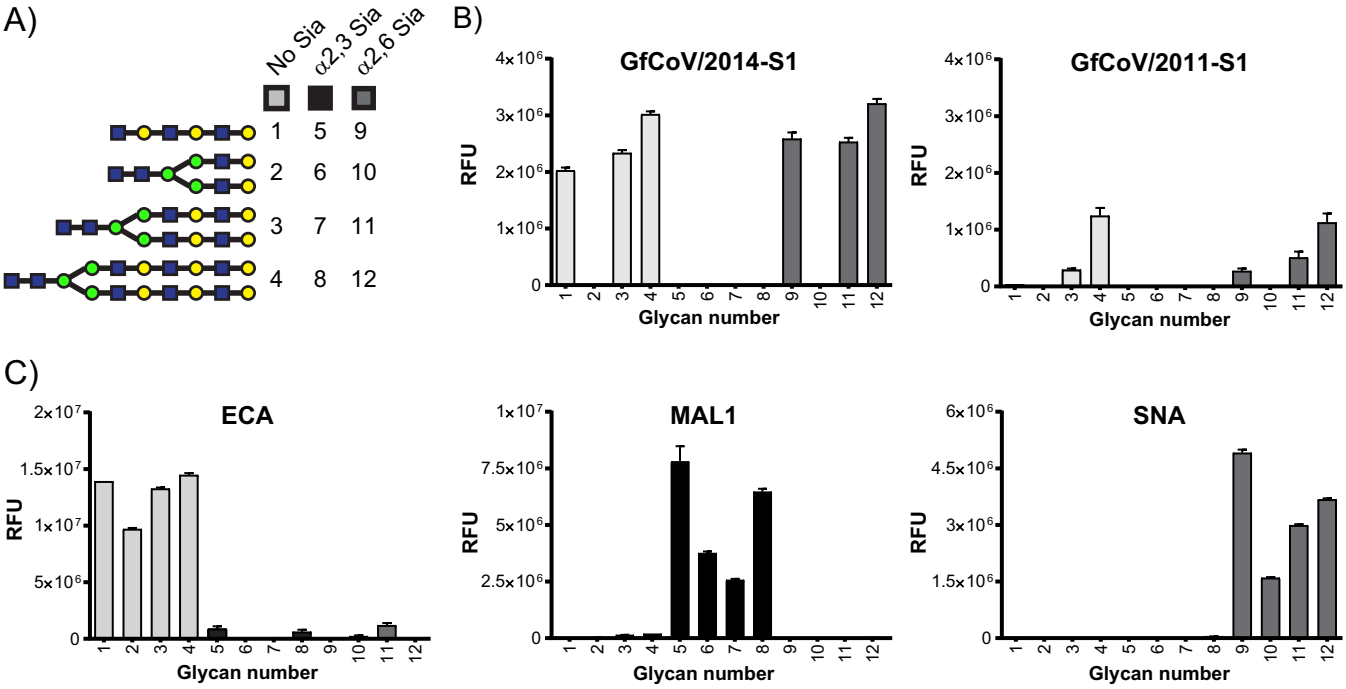


FIG 4 Glycan binding specificity of guinea fowl S1 proteins. (A) Schematic representation of selected glycan structures present on the glycan array; numbers correspond to those shown in the graphs. Numbers 1 to 4 represent glycans ending with galactose, numbers 5 to 8 represent glycans capped with alpha-2,3 -linked sialic acids, and numbers 9 to 12 represent glycans capped with alpha-2,6-linked sialic acids. Yellow circle, galactose; blue square, GlcNAc; green circle, mannose. (B and C) Glycan receptor specificity of GfCoV S1 proteins and lectins ECA, MAL1, and SNA in glycan array assay (Broszeit and de Vries, submitted). RFU, relative fluorescent units.

binding intensity of GfCoV/2011 S1 to glycans with terminal alpha-2,6 sialic acids was less than the binding intensity to glycans with terminal galactose (Fig. 5B, compare structures 3 and 4 to structures 11 and 12 at a protein concentration of 100 μg/ml to those at 20 μg/ml). This difference in preference for galactose-terminal glycans was not observed for GfCoV/2014 S1 since binding levels to glycan structures 3 and 4 and to structures 11 and 12 were similar in each dilution applied to the array (Fig. 5A). Taken together, the data indicate that GfCoV/2014 S1 has a higher affinity than GfCoV/2011 S1 for all glycans bound on the array.

GfCoV/2014 S1 has broader gastrointestinal tract tropism. To reveal whether the observed differences in glycan binding properties of the S1 proteins have biological consequences for tissue tropism, we first determined whether the identified glycans are indeed present on gastrointestinal tract tissues of healthy, uninfected guinea fowl. Both SNA and ECA lectins stained the epithelial lining of the duodenum, jejunum, and cecum intensely, while intermediate staining of the proventriculus and colon was observed. In the pancreas, only limited binding of SNA was observed, with no staining by ECA; in contrast, in the ileum ECA strongly bound whereas SNA bound only to a limited extent. In conclusion, all tissues of the gastrointestinal tract, except cloaca, express GfCoV glycan receptors (Table 2) (15).

Next, we investigated the binding patterns of GfCoV S1 proteins to gastrointestinal tissues. Both proteins stained the epithelial cells of almost the entire gastrointestinal tract (duodenum and colon in Fig. 6, first column; results are summarized in Table 2), indicating that receptors present on the tissues allow binding of S1. Interestingly, staining intensities of the lower intestinal tract (ileum, cecum, and colon) were much more apparent for GfCoV/2014 S1 than for GfCoV/2011 S1. This prompted us to analyze avidity and specificity of GfCoV S1 proteins to glycan receptors in the guinea fowl gastrointestinal tissues. We therefore pretreated tissue slides with *Arthrobacter ureafaciens* neuraminidase (AUNA) and/or galactosidase to cleave off terminal sialic acids and/or galactose residues from host glycans, respectively. Treatment of the tissues with

Downloaded from http://jvi.asm.org/ on April 22, 2021 at INRAE - Inst Natl de Rech pour l'Agriculture, l'Alimentation et l'Environnement

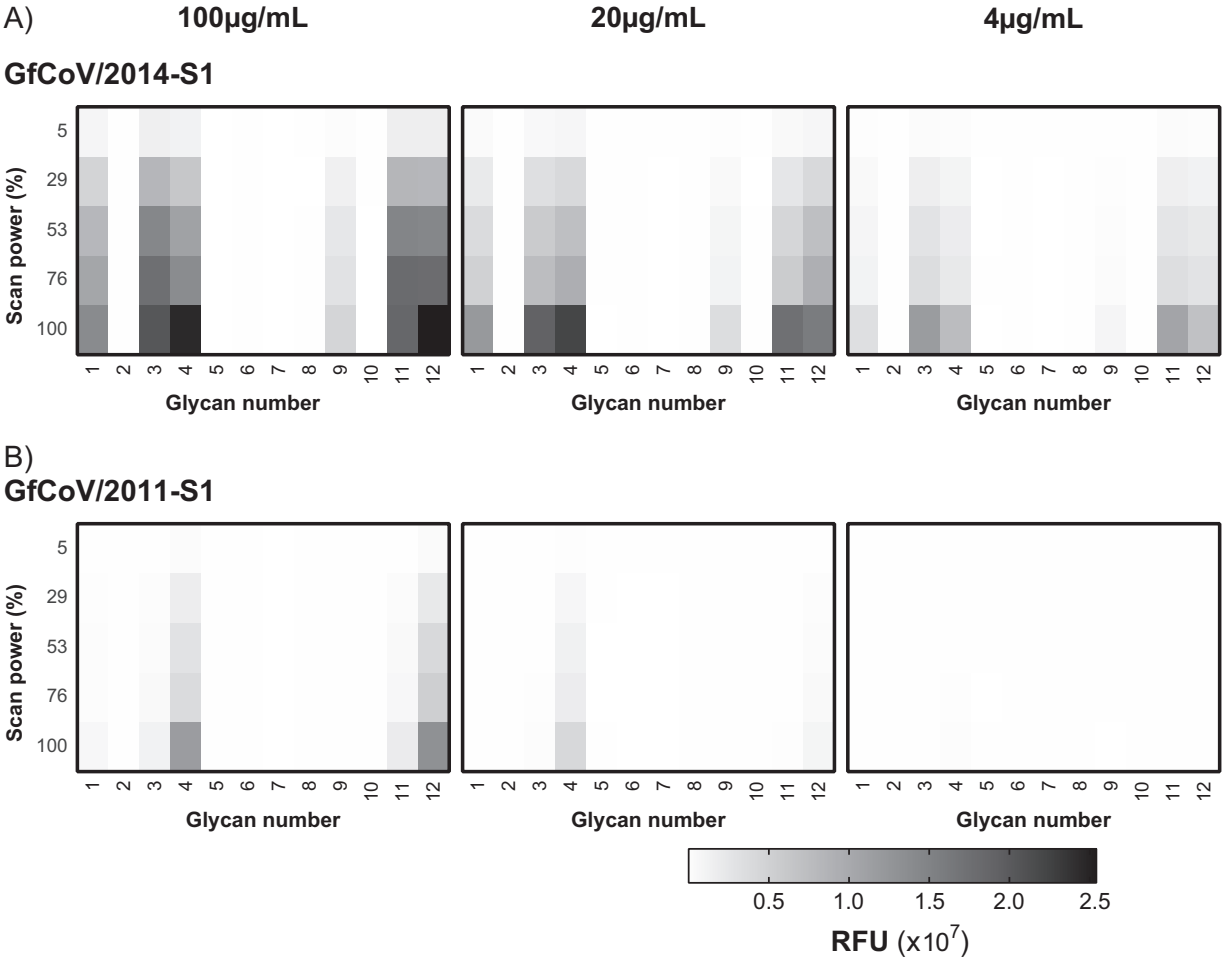


FIG 5 Glycan binding affinity of guinea fowl S1 proteins. (A and B) Glycan binding of GfCoV/2014 S1 and GfCoV/2011 S1 is shown as a heat map with 5-fold dilutions (100 μg/ml to 4 μg/ml) of the proteins applied to glycan array slides that were scanned at different laser intensities. RFU, relative fluorescent units. Glycan numbers correspond to schematic representations shown in Fig. 4A.

AUNA had only a minor effect on the binding of both GfCoV S1 proteins, with a slight decrease in binding intensity to the duodenum for GfCoV/2014 S1 (Fig. 6A, second column; Table 2). SNA lectin binding was completely abolished after pretreatment with AUNA, confirming that the treatment did effectively cleave off all sialic acids from the host glycans (Table 2).

When galactose residues were removed from the tissues by treatment with galactosidase prior to application of ECA, binding was severely reduced or totally absent

TABLE 2 Relative binding of viral proteins and lectins on guinea fowl intestinal tissues[a]

		GfCoV/2014-S1				GfCoV/2011-S1				ECA			SNA		
Treatment	AUNA	-	+	-	+	-	+	-	+	-	-	+	-	+	+
	Galactosidase	-	-	+	+	-	-	+	+	-	+	+	-	-	+
Tissue	proventriculus														
	duodenum														
	pancreas														
	jejunum														
	ileum														
	ceacum								na						
	colon														
	cloaca														

[a]Boxes are color coded as follows: white, no visible staining; gray, light to mild staining and/or not all epithelial cells show staining; black, intense staining with most of the epithelial cells showing positive signal. na, not analyzed.

Downloaded from http://jvi.asm.org/ on April 22, 2021 at INRAE - Inst Natl de Rech pour l'Agriculture, l'Alimentation et l'Environnement

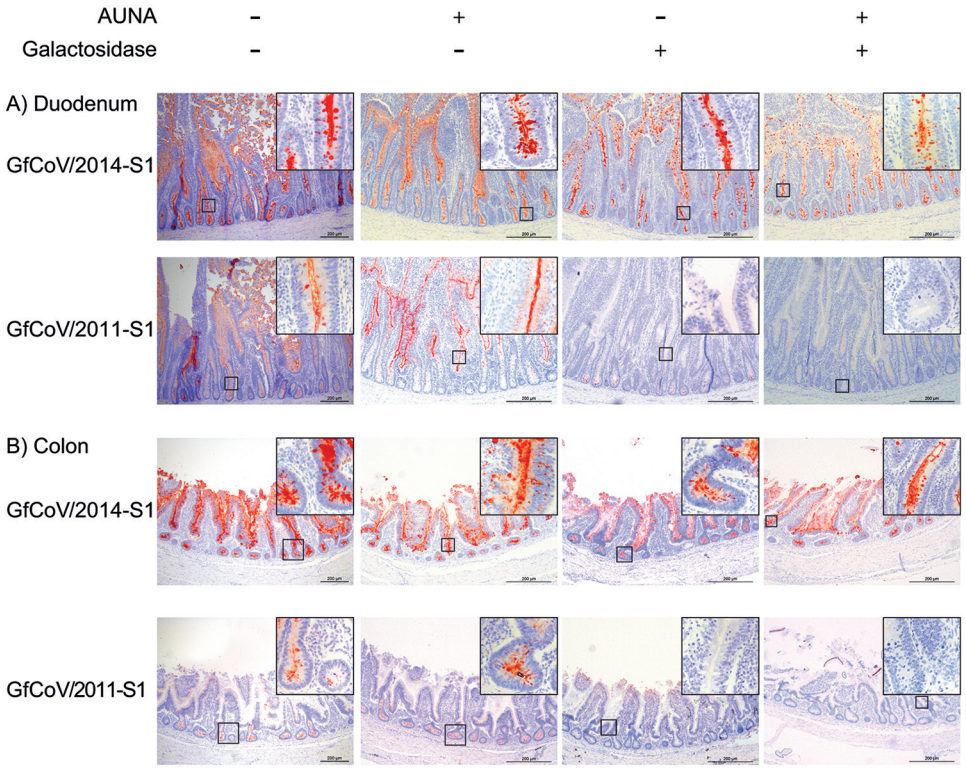


FIG 6 Binding of GfCoV S1 proteins to guinea fowl duodenum and colon without and with enzymatic pretreatment of the tissues. (A and B) Spike histochemistry was performed on uninfected, healthy duodenum and colon tissues without and with pretreatment of enzymes (AUNA and/or galactosidase) before application of GfCoV/2014 S1 and GfCoV/2011 S1. Binding of proteins was visualized by red staining.

(Table 2). Binding of GfCoV/2011 S1 to the tissue was completely abolished (Fig. 6, third column; Table 2), indicating that GfCoV tissue engagement is almost exclusively dependent on the presence of galactose-terminating glycans. On the other hand, GfCoV/2014 S1 still clearly bound to the epithelial cells of the intestinal tract, indicating a significant difference in receptor binding avidity (Fig. 6, third column; Table 2).

Finally, tissues were simultaneously pretreated with AUNA and galactosidase to remove both galactose and sialic acids from the glycans of the host. Indeed, binding levels of both ECA and SNA were strongly reduced (Table 2). Tissue binding of GfCoV/2011 S1 was completely prevented, while GfCoV/2014 S1 still clearly bound to the epithelial cells of the gastrointestinal tract (except pancreas) (Fig. 6, fourth column; Table 2). These results suggest that either a minor amount of receptor is still present or that an additional (glycan) receptor is involved in tissue binding of GfCoV/2014 S1.

DISCUSSION

In this study, we demonstrated ongoing GfCoV circulation in guinea fowl flocks in France. The sequence diversity between the viral attachment proteins of GfCoV circulating in 2011 and 2014 resulted in differences in receptor binding properties with profound phenotypic consequences. The relationship between these findings and *in vivo* pathogenesis can only be elucidated in detail, however, when new models to study this virus have been developed.

An amino acid sequence identity of 89% between viruses circulating only several years apart might indicate either that a novel GfCoV strain was introduced in France from a yet unidentified source or that there was high evolutionary pressure on the 2011 GfCoV strain. High mutation rates for avian coronaviruses are not uncommon (based on full-genome sequences, around 1.2×10^{-3} substitution/site/year [16, 17]). When the S1 sequences of GfCoV/2011 and GfCoV/2014-S1 are compared, the calculated mutation

Downloaded from http://jvi.asm.org/ on April 22, 2021 at INRAE - Inst Natl de Rech pour l'Agriculture, l'Alimentation et l'Environnement

rate was 5×10^{-2} substitutions/site/year with a ratio of nonsynonymous to synonymous substitutions (*dN*/*dS*) of 0.45. Similar mutation rates of the spike have been reported for IBV (18) and are believed to be driven by selective pressure after vaccination (19, 20). However, no vaccine is available against GfCoV or against the closely related turkey coronavirus, TCoV. Another driver for genetic diversity is the population size (21); however, this is unlikely to explain the observed high mutation rate of GfCoV since flocks are considerably smaller than chicken flocks. It might well be that circulating antibodies against field strains of GfCoV are the main drivers of the observed sequence diversity. Unfortunately, retrospective studies to further elucidate the contribution of virus evolution, the circulation of other virus populations in the last years, or the introduction of novel strains via, for example, trade of birds between farms are impossible due to the lack of archived material.

Here, we revealed a novel glycan receptor for GfCoV, the first coronavirus that binds N-glycans capped with alpha-2,6-linked sialic acids. Alpha-2,6 sialic acid presence has been reported previously in guinea fowl large intestine (15), along with the previously elucidated poly-LacNAc expressed in guinea fowl small intestine (4). Together, their expression patterns can explain in large part the tropism of GfCoV, but this observation, combined with the results presented in the manuscript, does not exclude the possibility that yet another host factor plays a role in GfCoV/2014 infection. Initial attempts to show whether protein receptors, required for infection of many other coronaviruses (22–24), are required have yet to be successful (data not shown).

While spike protein binding analyses suggest phenotypic differences between these viruses *in vivo*, the reported gross clinical signs in field cases between 2011 and 2014 were not markedly different. Unfortunately, and in contrast to a previous study (6), attempts to study the pathogenesis of GfCoV/2014 by inoculating commercial guinea fowls with GfCoV-containing fecal samples did not result in manifestations of clinical signs or convincing detection of viral RNA by reverse transcription-quantitative PCR (RT-QPCR) (data not shown). Whether this was due to previous exposure of commercial birds to GfCoV and, hence, circulating antibodies preventing the infection remains to be investigated.

Here, we have demonstrated that GfCoV/2014 S1 has higher affinity for glycan receptors and increased avidity for the lower gastrointestinal tract than GfCoV/2011 S1. The viral genetic diversity between these spikes and the implications for receptor recognition further add to our understanding of this virus for which models are basically lacking.

MATERIALS AND METHODS

Collection of field samples. Samples were collected from guinea fowls showing enteritis and concomitant high mortality (>10%) in flocks in five regions in France (Bretagne, Pays de Loire, Nouvelle-Aquitaine, Occitanie, and Auvergne-Rhône-Alpes) from February 2014 through November 2016. Gastrointestinal content was collected and stored at −80°C for viral RNA isolation. Tissues (duodenum, pancreas, air sac, lung, small intestine, large intestine, kidney, cloaca, trachea, and bursa) were collected during necropsy of euthanized or deceased animals in routine diagnostics by local veterinarians, fixed for 24 h in 4% (mass/vol) buffered formaldehyde, and stored in 70% ethanol.

Immunohistochemistry. Paraffin-embedded tissues were sliced at 4 μm, deparaffinized in xylene, and rehydrated in an ethanol gradient from 100% to 70%. Antigen retrieval was carried out in Tris-EDTA, pH 9.0 (preheated), before application of 1% H_2O_2 in methanol. After two washes in normal antibody diluent (Immunologic), the monoclonal antibody (MAb) mouse anti-IBV M protein 25.1 (Prionics, Lelystad, The Netherlands), cross-reacting with TCoV and GfCoV (5), was applied for 1 h at room temperature (RT). Slides were washed in phosphate-buffered saline (PBS)–0.1% Tween, and an EnVision kit (catalog no. K4001; Dako) was used for anti-mouse secondary antibody staining according to the manufacturer's protocol. Slides were washed three times in PBS, and viral M protein presence was visualized with aminoethylcarbazole (AEC). The tissues were counterstained with hematoxylin and mounted with AquaMount (Merck).

Molecular characterization of GfCoV. The gastrointestinal content collected from affected guinea fowl was clarified by centrifugation (30 s at 11,000 × *g*), and RNA was extracted using a Qiagen Viral RNA extraction kit according to the instructions of the manufacturer. A one-step real-time RT-PCR targeting the avian coronavirus N gene was carried out to confirm the presence of coronavirus RNA as previously described (13). Subsequently, the isolated RNA was reverse transcribed using a Revertaid kit with random hexamers (Thermo Fisher, Waltham, MA), and overlapping conventional PCRs were performed to amplify the guinea fowl S gene (primer sequences available upon request). Sanger sequencing of the resulting

Downloaded from http://jvi.asm.org/ on April 22, 2021 at INRAE - Inst Natl de Rech pour l'Agriculture, l'Alimentation et l'Environnement

fragments was performed using PCR primers. Contigs were generated with BioEdit (version 7.0.8.0) (25) and submitted to NCBI. MUSCLE (26) was used for the alignment, and MEGA (version 6.06) was used with a bootstrap value of 1,000 for the phylogeny (27). Selective pressure was calculated as *dN*/*dS*, and the hypothesis $dN = dS$ was tested using the Pamilo-Bianchi-Li method (28), with a P value of <0.05 considered statistically significant.

Construction of the expression vector. The codon-optimized sequence for GfCoV/2014 S1 (γCoV/AvCoV/guinea fowl/France/14032/2014), containing upstream NheI and downstream PacI restriction sites, was obtained from GenScript and cloned into the pCD5 expression vector by restriction digestion, as previously described (29). The S1 sequence is in frame with a C-terminal GCN4 trimerization motif and Strep-tag. The expression vector encoding GfCoV/2011 S1 was generated previously (29).

Production of recombinant proteins. Recombinant S1 proteins were expressed by transfection of human embryonic kidney (HEK293T) cells with pCD5 expression vectors using polyethylenimine (PEI) at a 1:12 (wt/wt) ratio. Cell culture supernatants were harvested after 6 days. The recombinant proteins were purified using Strep-Tactin Sepharose beads as previously described (29).

ELISA. Galβ1,4GlcNAcβ1,3Galβ1,4GlcNAc (Consortium for Functional Glycomics) was coated in a 96-well Nunc MaxiSorp plate (Sigma-Aldrich) at 0.5 μg/well overnight at 4°C, followed by blocking with 3% bovine serum albumin (BSA; Sigma) in PBS–0.1% Tween. S1 proteins were preincubated with Strep-Tactin–horseradish peroxidase (HRPO) (1:200) for 30 min on ice. For each protein, 2-fold dilutions were made in triplicate in PBS and applied onto the coated well, followed by incubation for 2 h at room temperature. TMB (3,3′,5,5′-tetramethylbenzidine; Thermo Scientific) substrate was used to visualize binding, after which the reaction was terminated using 1 M H_2SO_4. The optical density at 450 nm (OD_{450}) was measured in a FLUOstar Omega instrument (BMG Labtech), and MARS data analysis software was used for data analysis. Statistical analysis was performed using a two-way analysis of variance (ANOVA).

Glycan array. Glycan structures were printed in six replicates on glass slides (Nexterion Slide H; Schott Inc.). Prelabeled S1 proteins with Alexa Fluor 647-linked anti-Strep-tag mouse antibody and with Alexa Fluor 647-linked anti-mouse IgG (4:2:1 molar ratio) were applied to the slides (concentrations are given in figure legends) and incubated for 90 min, after which the slides were washed with PBS and deionized water, dried, and imaged immediately.

As controls different lectins were applied: *Erythrina crista-galli* agglutinin (ECA), which is specific for glycans with terminal galactose, *N*-acetylgalactosamine, or lactose, and *Sambuca nigra* agglutinin (SNA) and *Maackia Amurensis* lectin I (MAL1), which are specific for alpha-2,6-linked and alpha-2,3-linked sialic acids attached to terminal galactose, respectively. Of the six replicates, the highest and lowest values were removed, and of the remaining four replicates, the total signal values and standard deviations (SD) were calculated and plotted in bar graphs or heat maps.

Spike histochemistry. Spike histochemistry was performed as previously described (29). S1 proteins precomplexed with Strep-Tactin–HRPO were applied onto 4-μm sections of formalin-fixed paraffin-embedded healthy guinea fowl tissues, and binding was visualized using 3-amino-9-ethyl-carbazole (AEC; Sigma-Aldrich). Proteins were applied onto slides at 5 μg/ml. Where indicated (on Fig. 6, its legend, and the text), the tissues were treated per slide with 40 U β-galactosidase (β-Gal) (Megazyme, USA) or 2 mU of neuraminidase (sialidase) from *Arthrobacter ureafaciens* (AUNA) (Sigma, Germany) in 10 mM potassium acetate and 2.5 mg/ml Triton X-100, pH 4.2, and incubated at 40°C overnight (O/N) before protein application.

Lectin histochemistry. Lectin histochemistry was performed as previously described (4). Biotinylated *Erythrina crista-galli* lectin or biotinylated *Sambucus nigra* lectin (both from Vector Laboratories) were diluted in PBS to a final concentration of 2 μg/ml (ECA) or 6 μg/ml (SNA) and applied to healthy guinea fowl tissue sections for 30 min. After samples were washed with PBS, the signal was visualized by an avidin-biotin complex (ABC kit; Vector Laboratories) and counterstained with hematoxylin.

Data availability. Contigs are available in GenBank under accession numbers MG765535 to MG765542 and accession numbers MK290733 and MK290734.

ACKNOWLEDGMENTS

R.P.D.V. is a recipient of a VENI grant from the Netherlands Organization for Scientific Research (NWO); M.H.V is a recipient of a MEERVOUD grant from the NWO; and M.H.V. and M.F.D. are recipients of a Van Gogh collaboration grant from Nuffic.

REFERENCES

1. Duraes-Carvalho R, Caserta LC, Barnabe AC, Martini MC, Simas PV, Santos MM, Salemi M, Arns CW. 2015. Phylogenetic and phylogeographic mapping of the avian coronavirus spike protein-encoding gene in wild and synanthropic birds. Virus Res 201:101–112. https://doi.org/10.1016/j.virusres.2015.03.002.
2. Valastro V, Holmes EC, Britton P, Fusaro A, Jackwood MW, Cattoli G, Monne I. 2016. S1 gene-based phylogeny of infectious bronchitis virus: an attempt to harmonize virus classification. Infect Genet Evol 39:349–364. https://doi.org/10.1016/j.meegid.2016.02.015.
3. Circella E, Camarda A, Martella V, Bruni G, Lavazza A, Buonavoglia C. 2007. Coronavirus associated with an enteric syndrome on a quail farm. Avian Pathol 36:251–258. https://doi.org/10.1080/03079450701344738.
4. Ambepitiya Wickramasinghe IN, de Vries RP, Weerts EAWS, van Beurden SJ, Peng W, McBride R, Ducatez M, Guy J, Brown P, Eterradossi N, Gröne A, Paulson JC, Verheije MH. 2015. Novel receptor specificity of avian gammacoronaviruses that cause enteritis. J Virol 89:8783–8792. https://doi.org/10.1128/JVI.00745-15.
5. Brown PA, Courtillon C, Weerts E, Andraud M, Allee C, Vendembeuche A, Amelot M, Rose N, Verheije MH, Eterradossi N. 2018. Transmission kinetics and histopathology induced by European Turkey Coronavirus during experimental infection of specific pathogen free turkeys. Transbound Emerg Dis 66:234–242. https://doi.org/10.1111/tbed.13006.
6. Liais E, Croville G, Mariette J, Delverdier M, Lucas MN, Klopp C, Lluch J, Donnadieu C, Guy JS, Corrand L, Ducatez MF, Guerin JL. 2014. Novel

Downloaded from http://jvi.asm.org/ on April 22, 2021 at INRAE - Inst Natl de Rech pour l'Agriculture, l'Alimentation et l'Environnement

avian coronavirus and fulminating disease in guinea fowl, France. Emerg Infect Dis 20:105–108. https://doi.org/10.3201/eid2001.130774.
7. Le VB, Schneider JG, Boergeling Y, Berri F, Ducatez M, Guerin JL, Adrian I, Errazuriz-Cerda E, Frasquilho S, Antunes L, Lina B, Bordet JC, Jandrot-Perrus M, Ludwig S, Riteau B. 2015. Platelet activation and aggregation promote lung inflammation and influenza virus pathogenesis. Am J Respir Crit Care Med 191:804–819. https://doi.org/10.1164/rccm.201406-1031OC.
8. Jindal N, Mor SK, Goyal SM. 2014. Enteric viruses in turkey enteritis. Virus Dis 25:173–185. https://doi.org/10.1007/s13337-014-0198-8.
9. Casais R, Dove B, Cavanagh D, Britton P. 2003. Recombinant avian infectious bronchitis virus expressing a heterologous spike gene demonstrates that the spike protein is a determinant of cell tropism. J Virol 77:9084–9089. https://doi.org/10.1128/JVI.77.16.9084-9089.2003.
10. Promkuntod N, van Eijndhoven REW, de Vrieze G, Gröne A, Verheije MH. 2014. Mapping of the receptor-binding domain and amino acids critical for attachment in the spike protein of avian coronavirus infectious bronchitis virus. Virology 448:26–32. https://doi.org/10.1016/j.virol.2013.09.018.
11. Promkuntod N, Wickramasinghe IN, de Vrieze G, Grone A, Verheije MH. 2013. Contributions of the S2 spike ectodomain to attachment and host range of infectious bronchitis virus. Virus Res 177:127–137. https://doi.org/10.1016/j.virusres.2013.09.006.
12. Leyson C, Franca M, Jackwood M, Jordan B. 2016. Polymorphisms in the S1 spike glycoprotein of Arkansas-type infectious bronchitis virus (IBV) show differential binding to host tissues and altered antigenicity. Virology 498:218–225. https://doi.org/10.1016/j.virol.2016.08.030.
13. Maurel S, Toquin D, Briand FX, Queguiner M, Allee C, Bertin J, Ravillion L, Retaux C, Turblin V, Morvan H, Eterradossi N. 2011. First full-length sequences of the S gene of European isolates reveal further diversity among turkey coronaviruses. Avian Pathol 40:179–189. https://doi.org/10.1080/03079457.2011.551936.
14. Shang J, Zheng Y, Yang Y, Liu C, Geng Q, Luo C, Zhang W, Li F. 2018. Cryo-EM structure of infectious bronchitis coronavirus spike protein reveals structural and functional evolution of coronavirus spike proteins. PLoS Pathog 14:e1007009. https://doi.org/10.1371/journal.ppat.1007009.
15. Kimble B, Nieto GR, Perez DR. 2010. Characterization of influenza virus sialic acid receptors in minor poultry species. Virol J 7:365. https://doi.org/10.1186/1743-422X-7-365.
16. Hanada K, Suzuki Y, Gojobori T. 2004. A large variation in the rates of synonymous substitution for RNA viruses and its relationship to a diversity of viral infection and transmission modes. Mol Biol Evol 21:1074–1080. https://doi.org/10.1093/molbev/msh109.
17. Mahy BWJ. 2010. The evolution and emergence of RNA viruses. Emerg Infect Dis 16:899–899. https://doi.org/10.3201/eid1605.100164.
18. Lee CW, Jackwood MW. 2001. Origin and evolution of Georgia 98 (GA98), a new serotype of avian infectious bronchitis virus. Virus Res 80:33–39. https://doi.org/10.1016/S0168-1702(01)00345-8.
19. Kant A, Koch G, van Roozelaar DJ, Kusters JG, Poelwijk FA, van der Zeijst BA. 1992. Location of antigenic sites defined by neutralizing monoclonal antibodies on the S1 avian infectious bronchitis virus glycopolypeptide. J Gen Virol 73:591–596. https://doi.org/10.1099/0022-1317-73-3-591.
20. Zou N, Wang F, Duan Z, Xia J, Wen X, Yan Q, Liu P, Cao S, Huang Y. 2015. Development and characterization of neutralizing monoclonal antibodies against the S1 subunit protein of QX-like avian infectious bronchitis virus strain Sczy3. Monoclon Antib Immunodiagn Immunother 34:17–24. https://doi.org/10.1089/mab.2014.0081.
21. Toro H, van Santen VL, Jackwood MW. 2012. Genetic diversity and selection regulates evolution of infectious bronchitis virus. Avian Dis 56:449–455. https://doi.org/10.1637/10072-020212-Review.1.
22. Williams RK, Jiang GS, Holmes KV. 1991. Receptor for mouse hepatitis virus is a member of the carcinoembryonic antigen family of glycoproteins. Proc Natl Acad Sci U S A 88:5533–5536. https://doi.org/10.1073/pnas.88.13.5533.
23. Delmas B, Gelfi J, L'Haridon R, Vogel LK, Sjostrom H, Noren O, Laude H. 1992. Aminopeptidase N is a major receptor for the entero-pathogenic coronavirus TGEV. Nature 357:417–420. https://doi.org/10.1038/357417a0.
24. Li W, Moore MJ, Vasilieva N, Sui J, Wong SK, Berne MA, Somasundaran M, Sullivan JL, Luzuriaga K, Greenough TC, Choe H, Farzan M. 2003. Angiotensin-converting enzyme 2 is a functional receptor for the SARS coronavirus. Nature 426:450–454. https://doi.org/10.1038/nature02145.
25. Alzohairy A. 2011 BioEdit: an important software for molecular biology. GERF Bull Biosci 2:60–61.
26. Edgar RC. 2004. MUSCLE: multiple sequence alignment with high accuracy and high throughput. Nucleic Acids Res 32:1792–1797. https://doi.org/10.1093/nar/gkh340.
27. Tamura K, Stecher G, Peterson D, Filipski A, Kumar S. 2013. MEGA6: Molecular Evolutionary Genetics Analysis version 6.0. Mol Biol Evol 30:2725–2729. https://doi.org/10.1093/molbev/mst197.
28. Pamilo P, Bianchi NO. 1993. Evolution of the Zfx and Zfy genes: rates and interdependence between the genes. Mol Biol Evol 10:271–281. https://doi.org/10.1093/oxfordjournals.molbev.a040003.
29. Wickramasinghe IN, de Vries RP, Grone A, de Haan CA, Verheije MH. 2011. Binding of avian coronavirus spike proteins to host factors reflects virus tropism and pathogenicity. J Virol 85:8903–8912. https://doi.org/10.1128/JVI.05112-11.

Downloaded from http://jvi.asm.org/ on April 22, 2021 at INRAE - Inst Natl de Rech pour l'Agriculture, l'Alimentation et l'Environnement